July 2018

Optimal Dispatch Controller For Fuel Cell Integrated Building

Yashen Lin
National Renewable Energy Laboratory, United States of America, yashen.lin@nrel.gov

Dustin McLarty
School of Mechanical and Materials Engineering, Washington State University, dustin.mclarty@wsu.edu

Annabelle Pratt
National Renewable Energy Laboratory, United States of America, Annabelle.Pratt@nrel.gov

Brian Ball
National Renewable Energy Laboratory, United States of America, Brian.Ball@nrel.gov

Gregor Henze
National Renewable Energy Laboratory, United States of America; Department of Civil, Environmental, and Architectural Engineering, University of Colorado Boulder, gregor.henze@colorado.edu

See next page for additional authors

Authors
Yashen Lin, Dustin McLarty, Annabelle Pratt, Brian Ball, Gregor Henze, and Genevieve Saur

Optimal Dispatch Controller for Fuel Cell-Integrated Building

Yashen Lin[1*], Dustin McLarty[2], Annabelle Pratt[1], Brian Ball[1], Gregor Henze[1,3], Genevieve Saur[1]

[1] National Renewable Energy Laboratory,
Golden, CO, USA
{yashen.lin / annabelle.pratt / brian.ball/ genevieve.saur}@nrel.gov

[2] Washington State University, School of Mechanical and Materials Engineering,
Pullman, WA, USA
dustin.mclarty@wsu.edu

[3] University of Colorado Boulder, Department of Civil, Environmental, and Architectural Engineering,
Boulder, CO, USA
gregor.henze@colorado.edu

* Corresponding Author

ABSTRACT

Stationary fuel cells can generate both electrical power and heat, making them a promising local source to serve building loads. In this paper, we develop an optimal energy dispatch controller to operate a fuel cell-integrated building. The controller leverages the inherent thermal storage in the building to reduce its operating cost and to allow the building to participate in providing grid services. The proposed controller is tested in a co-simulation setup, where the real building is represented as a high-fidelity model in EnergyPlus.

1. INTRODUCTION

Buildings contribute to around 40% of the total energy consumption in the United States (U.S. Department of Energy, 2011). Improvements to building operation offer substantial economic benefits and emissions reductions. Opportunities arise as more renewable energy sources are integrated into the electric power grid, and the inherent flexibility that buildings can provide becomes a valuable asset for grid services (Ipakchi and Albuyeh, 2009). Stationary fuel cells providing combined heat and power (CHP) add more flexibility to building operation, where both significant electrical and thermal loads need to be met. As the technology matures, improved fuel cell responsiveness allows for advanced dynamic applications to maximize their utility within the building system.

The integration of fuel cells and battery energy storage systems (BESS) to buildings presents several challenges and opportunities for the optimal management of resources. In this work, we develop an optimal energy dispatch controller (EDC) for the real-time management of a fuel cell-integrated building system. The objective is to minimize building operating costs and maximize profits from participating in electric power grid ancillary service markets while maintaining occupant comfort.

To achieve this objective, we develop a specially tailored model predictive control (MPC) algorithm to schedule the operation of a fuel cell, a BESS, and building equipment in response to a time-of-use electricity tariff and an ancillary services price. The controller determines the optimal schedules during a 24-hour horizon according to weather and building load forecasts. This optimal schedule is implemented for a 1-hour period. Measurements from the fuel cell-integrated building are collected and used to update the optimization for the next 24-hour period. This recursive update ensures that the algorithm is robust to forecast errors and model mismatch. The effectiveness of the proposed algorithm is demonstrated with a co-simulation setup, where the building is represented as a high-fidelity model in the EnergyPlus building simulation program and the optimal control is implemented in MATLAB.

The proposed EDC provides a tool to manage the real-time operation of a fuel cell-integrated building. It also helps building operators and the fuel cell industry assess the potential benefits of integrating stationary fuel cells with buildings.

The rest of the paper is organized as follows. Section 2 provides an overview of the control architecture. Section 3 presents the system modeling. Section 4 describes the optimization problem formulation, which is the core of the proposed EDC. Section 5 presents the co-simulation setup and simulation results. Section 6 concludes the paper and outlines future work directions.

2. Control Architecture

2.1 System Architecture

In this section, we provide an overview of the system we studied in this work, which includes the building and its heating, ventilation and air conditioning (HVAC) system; fuel cell; and battery storage. Figure 1 shows a schematic of the system architecture. In this work, we focus on a variable air volume (VAV) HVAC system, which is common in large commercial buildings (U.S. Energy Information Administration, 2012). There are several loops in the system: the air loop, the heating hot water loop, and the chilled water loop. In the air loop, the return air from the zones is recirculated and mixed with outdoor air; the mixed air then passes through the coiling coil, where it is cooled and dehumidified; the conditioned air is then supplied to the terminal VAV boxes, where the air is reheated if needed to maintain comfortable indoor climate. In the chilled water loop, chilled water is produced at the chiller and delivered to the cooling coil to condition the air. In the heating hot water loop, the hot water is produced by the boiler and fuel cell and delivered to the heating coils.

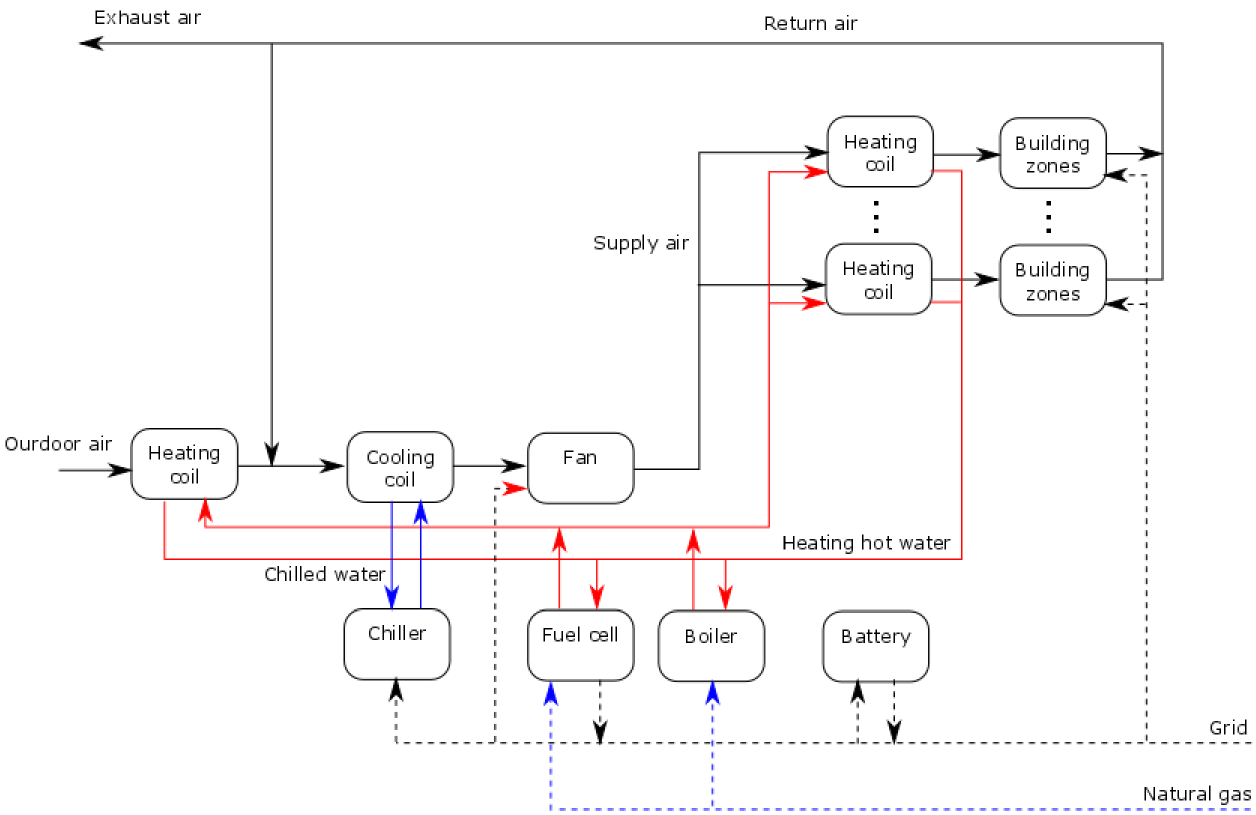

Figure 1. Schematic of the system studied in this work. The black solid line is the air loop. The red solid line is the heating hot water loop. The blue solid line is the chilled water loop. The black dotted line describes the electric connection. The blue dotted line describes the natural gas connection.

2.2 Energy Dispatch Controller

Buildings have both significant electrical load and thermal load, making them ideal customers for CHP systems, such as fuel cells. The flexibility embedded in building thermal inertia provides more potential to use the full capacity of the CHP. In this work, we developed the EDC to optimize the operation of the fuel cell, BESS, and building HVAC system. We adopted MPC as the control method, which uses dynamic models to predict the behavior of the studied system and optimize over a prediction horizon (Camacho and Alba, 2013). MPC is ideal for our task because it takes future time steps into consideration so we can use the flexibility of buildings. It is also capable of handling constraints in the system.

In the EDC, we schedule the zone temperature set point, fuel cell operation, battery charging and discharging, and ancillary service participation. The EDC follows the following steps:

1. At hour k, solve an optimization problem to decide the system operation schedule for the next 24-hour scheduling period using the system model and forecast (load, weather, prices set by the market).
2. Pass the optimal schedule to the low-level building automation controllers and implement the schedule for a 1-hour implementation period.
3. At hour k+1, collect the actual measurements from the building and update the forecast.
4. Repeat 1 through 3.

Formulating the scheduling optimization problem is the key in the EDC. Both accuracy and complexity need to be considered. In this work, we formulate the scheduling problem as a mixed-integer linear programing problem, which can be solved efficiently with established solvers. Details about the system modeling and optimization problem formulation are presented in the following sections.

3. System Modeling

3.1 Reduced-Order Model for Building Thermal Dynamics

The thermal dynamics of the building are an important part of the system. They describe how the zone temperatures evolve with heat gains. In this work, we adopt the well-known RC network model (Gouda *et al.*, 2002). In the model, the thermal dynamics are represented using an electrical circuit. Voltage represents temperature, current represents heat gain, and resistance and capacitance represent thermal resistance and capacitance. The zone can be modeled with different numbers of Rs and Cs. More Rs and Cs provide better accuracy while also making the model more complicated. In this work, we use a reduced-order model (ROM) that consists of a 2R-1C model for the surface and an additional C for the zone thermal mass (Lin *et al.*, 2012). For demonstration in this paper, we focus on a single zone model. The model can be readily extended to multizone buildings. The thermal dynamics are given by the following equations:

$$C_z \dot{T}_z = \frac{1}{R_1}(T_w - T_z) + \dot{m} C_{pa}(T_s - T_z) + P_{lh} + P_{rh}$$

$$C_w \dot{T}_w = \frac{1}{R_1}(T_z - T_w) + \frac{1}{R_2}(T_{oa} - T_w)$$

where the two states are zone temperature, T_z, and wall temperature, T_w; $\dot{m}$ is the supply airflow rate; T_s is the supply air temperature; P_{lh} is the heat gain into the zone (solar, occupancy, etc.); P_{rh} is the reheat from the HVAC system; and T_{oa} is the outdoor air temperature. Discretizing the system with Euler method, we get:

$$T_{z,k+1} = T_{z,k} + \frac{\Delta t}{C_z}\left[\frac{1}{R_1}\left(T_{w,k} - T_{z,k}\right) + \dot{m}_k C_{pa}\left(T_s - T_{z,k}\right) + P_{lh,k} + P_{rh,k}\right]$$

$$T_{w,k+1} = T_{w,k} + \frac{\Delta t}{C_w}\left[\frac{1}{R_1}\left(T_{z,k} - T_{w,k}\right) + \frac{1}{R_1}\left(T_{oa,k} - T_{w,k}\right)\right]$$

where Δt is the time step. Note that the second term in the T_z dynamics has a bilinear term with multiplication of $\dot{m}$ and T_z. These two variables are both decision variables in the optimization problem, resulting in a non-convex problem. To simplify the optimization problem formulation, we assume that, in calculating this term, T_z takes a constant value. The reasoning behind this is that the zone temperature is maintained within a temperature range, so the difference between the actual T_z and a constant set point is reasonably small. We note that this simplifying assumption is only applied in this calculation, and T_z remains a state variable in other parts of the problem formulation.

3.2 Equipment Modeling

In this work, we consider a generic model for the fuel cell, which consumes natural gas and generates electricity and heat. Let the fuel consumption of the fuel cell (in the unit of power) be $P_{fc,f}$, then the output of the fuel cell is given by:

$$P_{fc,e} = \eta_e P_{fc,f}$$
$$P_{fc,h} = \eta_h P_{fc,f}$$

where η_e is the electric efficiency and η_h is the heat efficiency. We assume that the fuel cell operates in electric following mode, which means that all electric power generated by the fuel cell will be used by the building and the heat generated can be used or rejected. The dynamics of the fuel cell are modeled by a fixed ramp rate limit. We also consider a minimum up time and a minimum down time, which means that the fuel cell needs to stay on for a period of time once it is started up and it needs to stay off for a period of time once it is shut down. There are costs associated with the start-up and shutdown.

In the chilled water loop, the chiller provides the cooling needed. The air is conditioned at the cooling coil. The heat taken out of the air is given by:

$$P_{cc} = \dot{m} C_p (T_{mix} - T_s)$$

where $T_{mix} = \alpha T_{oa} + (1 - \alpha) T_z$, where α is the outdoor air ratio. We do not model the dynamics of the cooling coil and chiller. The chiller power is given by:

$$P_{ch} = \frac{1}{\eta_{COP}} P_{cc}$$

where η_{COP} is the coefficient of performance of the chiller. Note that we do not consider latent load in this work.

In the heating hot water loop, the heat needed is provided by the fuel cell and boiler, i.e.:

$$P_{rh} = P_{fc,h} + P_{boil}$$

We do not model the dynamics in the heating equipment. The fuel cell heat output is determined by the scheduling problem, and the rest of heat needed by the building is provided by the boiler.

The fan power is modeled as a linear function of the airflow rate to keep the optimization problem convex, i.e.:

$$P_f = a_f \dot{m} + b_f$$

where a_f and b_f are fan coefficients.

The battery is characterized by its charging efficiency, η_c, and discharging efficiency, η_d, i.e.:

$$E_{bat,k+1} = E_{bat,k} + \eta_c P_{bat,in} - \frac{1}{\eta_d} P_{bat,out}$$

where E_{bat} is the state of charge of the BESS, and $P_{bat,in}$ and $P_{bat,out}$ are the battery charging and discharging. The charging and discharging are modeled as separate decision variables. Because simultaneous charging and discharging leads to energy loss and increased cost, the optimal solution will minimize simultaneous charging and discharging.

4. Optimization Problem Formulation

The scheduling optimization problem is the core of the EDC. In simplified terms, we want to find the temperature set points and corresponding equipment operation that gives us the lowest cost. In this section, we present the formal optimization problem formulation in detail.

4.1 Objective Function

The objective of the optimization problem is to minimize the electricity and natural gas bill and maximize the payment from grid services. The objective function is defined as:

$$J = \sum_t J_{e,t} + J_{ng,t} + J_{uc,t} - J_{as,t}$$

where J_e and J_{ng} are the costs of electricity and natural gas, J_{uc} is the cost for the fuel cell start-up and shutdown, and J_{as} is the payment for providing ancillary service to the power grid.

The electricity cost is determined by the power consumed from the grid:

$$J_e = c_e P_e$$

where c_e is the electricity price, and P_e is the power consumption from the grid, which is calculated by:

$$P_e = P_{ch} + P_f + P_{le} + P_{bat,in} - P_{fc,e} - P_{bat,out}$$

where P_{le} is the uncontrollable building electric loads.

Similarly, the natural gas cost is given by:

$$J_{ng} = c_{ng} P_{ng}$$

where c_{ng} is the natural gas price, and P_{ng} is calculated by:

$$P_{ng} = P_{fc,f} + P_{boil}$$

The fuel cell unit commitment cost is given by:

$$J_{uc} = c_{up} w_{up} + c_{down} w_{down}$$

where c_{up} and c_{down} are startup and shut down cost, w_{up} and w_{down} are binary variables indicating whether the fuel cell is turned on or shut down at each time step.

We consider a generic model for ancillary services. Let R_{as} be the power capacity reserved for provision of ancillary services, and c_{as} be the ancillary service price. The ancillary service payment is given by:

$$J_{as} = c_{as} R_{as}$$

Additional constraint is added to capture the impacts of providing ancillary services; see Section 4.4 for details.

4.2 Decision Variables

The core decision variables are:

$$u = \left[T_{set}, \dot{m}, P_{rh}, P_{fc,f}, P_{fc,hb}, w_{fc}, P_{bat,in}, P_{bat,out}, R_{as}\right]^T$$

which includes HVAC operation ($T_{set}, \dot{m}, P_{rh}$), fuel cell operation ($P_{fc,f}, P_{fc,hb}, w_{fc}$), battery charging and discharging ($P_{bat,in}, P_{bat,out}$), and ancillary service participation (R_{as}). Note that T_{set} is the zone temperature set point, $P_{fc,hb}$ is the portion of heat generated by the fuel cell that is used by the building, and w_{fc} is the binary variable for fuel cell on/off status.

4.3 Optimization Problem

Consider a general MPC problem, where the system model is described as:

$$x_{k+1} = f(x_k, u_k, d_k)$$

where x are the state variables, u are the control variables, and d are the exogenous inputs. The constraints on the state variables and control variables are given by:

$$h(x_k, u_k, d_k) \leq 0$$
$$g(x_k, u_k, d_k) = 0$$

To facilitate the optimization problem formulation, we consider the state variable x as a decision variable as well. The optimization problem can then be written as:

$$\begin{aligned} \min_{x,u} \quad & J(x, u, d) \\ s.t. \quad & x_{k+1} = f(x_k, u_k, d_k) \\ & h(x_k, u_k, d_k) \leq 0 \\ & g(x_k, u_k, d_k) = 0 \end{aligned}$$

In our EDC, the objective function J is given in Section 4.1. The state variables x are the zone temperature, the wall temperature and BESS state of charge (SOC), and the function f includes the thermal dynamics (described in Section 3.1) and BESS SOC dynamics (described in section 3.2). The control variables are discussed in Section 4.2. The exogenous inputs include weather, occupancy loads, etc. The other constraints are detailed in the next section.

4.4 Constraints

To capture the relationship between the temperature set points, HVAC operation, and the actual temperature dynamics, we assume that the actual temperature achieves the set point at the next scheduling time step. The reason behind this is that the HVAC system reacts to the set point in a faster timescale than the scheduling timescale, so by the end of the scheduling time step, the HVAC system has driven the actual temperature to the set point. This assumption is enforced by the following constraint:

$$T_{z,k+1} = T_{set,k}$$

This constraint links the temperature set points to the rest of the system.

Suppose the fuel cell has a minimum run time τ_{up} and a minimum down time τ_{down}. Let w_{fc} be the binary variables to capture the on/off status of the fuel cell. The minimum run time and minimum down time constraints can be written as:

$$-w_{fc,k-1} + w_{fc,k} - w_{fc,j} \leq 0, \forall j \in \{k+1, \cdots, k+\tau_{up}\}$$
$$w_{fc,k-1} - w_{fc,k} + w_{fc,j} \leq 0, \forall j \in \{k+1, \cdots, k+\tau_{down}\}$$

To facilitate the unit commitment cost calculation, we define the binary variables w_{up} and w_{down} to describe whether the fuel cell is turned on or shut down at each time step. This is achieved by the objective function and the following constraints:

$$-w_{fc,k-1} + w_{fc,k} - w_{up} \leq 0$$
$$w_{fc,k-1} - w_{fc,k} - w_{down} \leq 0$$

The equipment limits are given by:

$$w_{fc}P_{fc,min} \leq P_{fc,f} \leq w_{fc}P_{fc,max}$$
$$-P_{fc,ramp} \leq P_{fc,f,k+1} - P_{fc,f,k} \leq P_{fc,ramp}$$
$$E_{bat,min} \leq E_{bat} \leq E_{bat,max}$$
$$P_{bat,min} \leq P_{bat,in} \leq P_{bat,max}$$
$$P_{bat,min} \leq P_{bat,out} \leq P_{bat,max}$$
$$\dot{m}_{min} \leq \dot{m} \leq \dot{m}_{max}$$
$$P_{fc,hb} \leq P_{fc,h}$$
$$R_{as,min} \leq R_{as} \leq R_{as,max}$$

where the first constraint is the fuel cell capacity limit, the second is the fuel cell ramping constraint, the next is the battery energy capacity, the next two are the battery power capacity, the next is the supply airflow rate limit, the next one ensures that the heat used by the building from the fuel cell cannot exceed the total heat generated by the fuel cell, and the last is the limit for the ancillary service participation, which is determined by market regulation and user preference.

The BESS SOC is constrained to return to the initial value at the end of the scheduling horizon, i.e.:

$$E_{bat,N} = E_{bat,0}$$

This is to capture the potential benefits of having energy stored beyond the scheduling horizon.

The zone temperature is bounded by a comfortable range as follows:

$$T_{min} + T_{as} \leq T_z \leq T_{max} - T_{as}$$

where T_{as} is a temperature buffer for providing ancillary services. The reason behind this is that when the building provides ancillary service, the power consumption deviates from the scheduled value, causing the actual zone temperature to deviate from the scheduled value as well. The temperature buffer is added to ensure that the actual zone temperature remains in the original comfortable range when the grid requests ancillary services. In this work, we define T_{as} as follow:

$$T_{as} = k_{as}R_{as}$$

To this end, we have formulated a mixed-integer linear programing problem for the EDC, which can be solved efficiently by established optimization problem solvers. In this work, Gurobi is used as the solver.

5. Simulation Study

5.1 Simulation Setup

To demonstrate the performance of the EDC, we developed a co-simulation framework, which is shown in Figure 2. EnergyPlus is used to represent the actual building behavior. MLE+ serves as the interface between EnergyPlus and MATLAB where the EDC codes reside (Bernal *et al.*, 2012). As discussed in Section 2.2, the EDC solves the scheduling problem for the next 24-hour horizon using an MPC approach that relies on a system model, and sends the optimal schedule to the building, where it gets implemented for 1 hour. Measurements from the buildings are collected to update the forecast of the uncontrollable load and the internal heat gain by the forecasting module. The forecasting module is currently calculated based on the schedule information in the EnergyPlus model. The updated information is used by the EDC to run the optimization problem for the next time period. Weather and market information is provided to the EnergyPlus building model (through MLE+) and to the EDC.

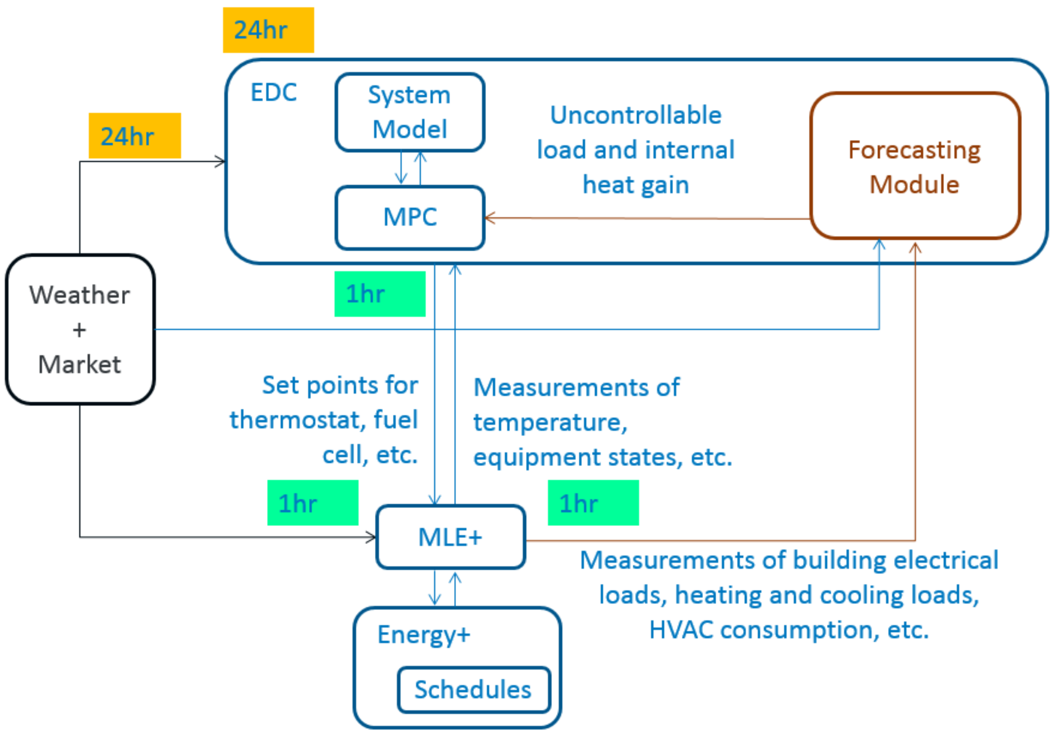

Figure 2. Schematic of the co-simulation setup.

In this work, we demonstrate the EDC with a modified large office building from the DOE commercial reference buildings (Deru *et al.*, 2011). We reduced the building to a single zone by removing the floors other than the ground (first) floor and collapsed the zones on the ground floor into a single zone, while keeping the equipment and material types the same. The location of the building is chosen to be in the Washington, D.C. area because it requires significant reheating during the winter and significant dehumidification during the summer so that the heat from the fuel cell can be used.

To calibrate the ROM parameters (C_z, C_w, R_1 and R_2), we ran a 1-year EnergyPlus simulation and collected the input and output data. The RC values are calibrated through a system identification process and are listed along with other parameters used in the simulation in Table 1.

Table 1. Parameters in the simulation study.

C_z	C_w	R_1	R_2	η_{COP}	η_c	η_d
5e6 J/K	3.75e8 J/K	0.03e-3 K/W	0.59e-3 K/W	3.5	0.9	0.9
$\eta_{fc,e}$	$\eta_{fc,h}$	k_{as}	T_{min}	T_{max}	$P_{fc,min}$	$P_{fc,max}$
0.5	0.35	1e-4 K/W	21 ºC	23 ºC	10 kW	50 kW
$P_{fc,ramp}$	$E_{bat,max}$	$P_{bat,max}$	$\dot{m}_{min}$	$\dot{m}_{max}$	τ_{up}	τ_{down}
25 kW	10 kWh	10 kW	2.23 kg/s	10 kg/s	6 h	6 h

5.2 Simulation Results

We compared three cases in our co-simulation: (i) with EDC and fuel cell; (ii) with EDC, no fuel cell; (iii) no EDC, no fuel cell, and temperature set point constant. Comparing (i) and (ii) shows the impact of adding a fuel cell into the system with the EDC; comparing (ii) and (iii) shows the impact of the EDC when there is no fuel cell; comparing (i) and (iii) shows the total benefits of adding the EDC and a fuel cell. We also studied two pricing scenarios: (a) low natural gas price; (b) high natural gas price. In both pricing scenarios, electricity prices peak from 16:00 to 20:00 every day, and natural gas and ancillary services have a flat price. Results from a 7-day simulation during wintertime are shown in Figure 3, Table 2, and Table 3.

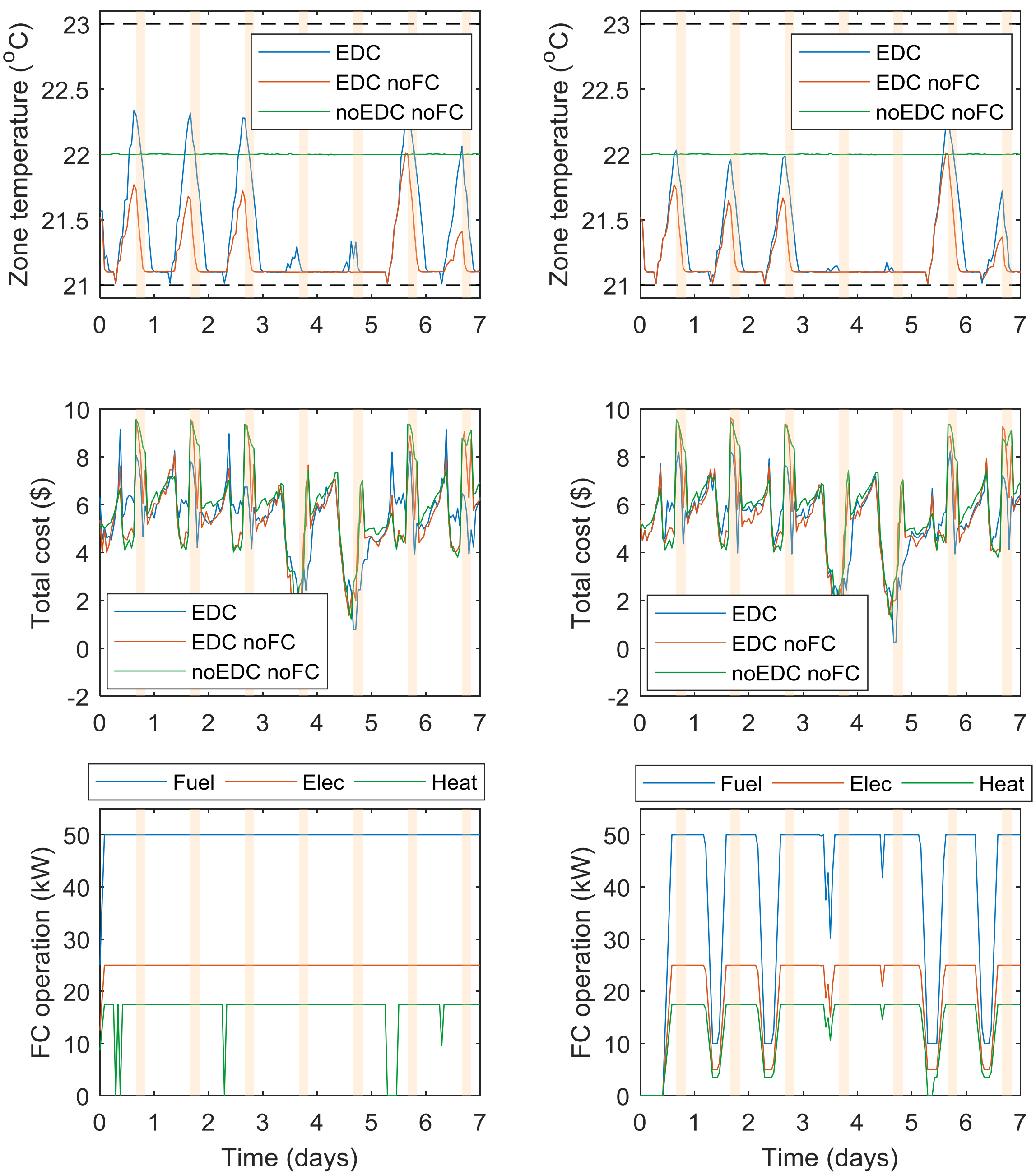

Figure 3. Co-simulation results. The left column is for the low natural gas price scenario, and the right column is for the high natural gas price scenario. The first row shows zone temperature, the middle row shows the total cost, and the bottom row shows the fuel cell (FC) operation.

Table 2. Simulation results in the low natural gas price scenario (unit in $).

	Total cost	Electricity cost	NG cost	AS payment
EDC (case i)	398	81	321	5
EDC, no FC (case ii)	733	611	127	5
No EDC, no FC (case iii)	747	594	153	

Table 3. Simulation results in the high natural gas price scenario (unit in $).

	Total cost	Electricity cost	NG cost	AS payment
EDC (case i)	914	182	736	5
EDC, no FC (case ii)	946	612	338	5
No EDC, no FC (case iii)	1003	594	409	

There are several observations from the simulation results. In the low natural gas price scenario, it is cheaper to run the fuel cell even if only the electricity is used by the building. Thus, as shown in Figure 3, bottom left, the fuel cell runs at full capacity almost all the time, and the heat is rejected during certain time periods when the building does not have enough heating load. Naturally, as shown in Table 2, there is a significant cost savings when we add the fuel cell to the system. In the high natural gas price scenario, however, it is only economical to run the fuel cell when both the electricity and heat are used by the building. When the building does not have enough heating load, it is better to obtain power from the grid rather than from the fuel cell. This is evident from Figure 3, bottom right, where the fuel cell reduces its output during periods with low building heating load. Higher natural gas price also reduces the cost savings of adding the fuel cell to the system, as shown in Table 3. The difference between the two pricing scenarios in cost savings can also be observed from the middle plots in Figure 3, where the difference between the cases are more significant in the low natural gas price scenario.

In both price scenarios, for most of the time, the EDC keeps the temperature close to the lower limits to reduce heating. It also allows the temperature to float higher when the building does not need heating from the HVAC system. It keeps the temperature a little higher than the lower limit to secure the buffer for providing ancillary services. This is shown in the top plots in Figure 3. However, the savings of using the EDC without the fuel cell is small in both scenarios. This is most likely caused by model mismatch. The EDC uses the calibrated ROM to predict the behavior of the building. Because the ROM cannot perfectly capture the dynamics of the building, the EDC prediction also has some error. When the EDC set points are implemented in the "real building" in EnergyPlus, the actual power consumption of the equipment is different from what the EDC expected, leading to a suboptimal performance. Improving the ROM is a direction for future work to improve the EDC performance.

6. CONCLUSIONS

Stationary fuel cells are a promising alternative for serving building electricity and heating loads. In this paper, we developed the EDC to operate the fuel cell, building HVAC system, and the BESS. We tested the EDC in a co-simulation setup, where the real building behavior is represented by a high-fidelity EnergyPlus simulation. We demonstrated that the fuel cell has the potential to significantly reduce the building operating cost. The magnitude of the cost savings depends on market prices and model accuracy.

There are several avenues for future research that our team will pursue. One direction is to investigate the impact of model mismatch on the EDC. We are working on methods to improve the ROM to better present the building behavior. We will study the benefits of adding thermal storage to the system. We will also add more realistic market pricing scenarios—for example, adding demand charges. The optimal dispatch controller will also be integrated into a tool that is under development to determine the optimal sizing for the fuel cell and energy storage devices.

REFERENCES

U.S. Department of Energy. (2011). *Buildings energy data book*. Retrieved from https://openei.org/doe-opendata/dataset/buildings-energy-data-book

Ipakchi, A., & Albuyeh, F. (2009). Grid of the future. *IEEE power and energy magazine*, *7*(2), 52-62.

U.S. Energy Information Administration. (2012). *Commercial buildings energy consumption survey (CBECS).* Retrieved from https://www.eia.gov/consumption/commercial/

Camacho, E. F., & Alba, C. B. (2013). *Model predictive control.* Springer Science & Business Media.

Gouda, M. M., Danaher, S., & Underwood, C. P. (2002). Building thermal model reduction using nonlinear constrained optimization. *Building and environment*, *37*(12), 1255-1265.

Lin, Y., Middelkoop, T., & Barooah, P. (2012). Issues in identification of control-oriented thermal models of zones in multi-zone buildings. *Decision and Control (CDC), 2012 IEEE 51st Annual Conference on* (6932-6937). IEEE.

Bernal, W., Behl, M., Nghiem, T. X., & Mangharam, R. (2012). MLE+: a tool for integrated design and deployment of energy efficient building controls. *Proceedings of the Fourth ACM Workshop on Embedded Sensing Systems for Energy-Efficiency in Buildings* (123-130). ACM.

Deru, M., Field, K., Studer, D., Benne, K., Griffith, B., Torcellini, P., Liu, B., Halverson, M., Winiarski, D., Rosenberg, M. & Yazdanian, M. (2011). *U.S. Department of Energy commercial reference building models of the national building stock.* Retrieved from https://www.nrel.gov/docs/fy11osti/46861.pdf

ACKNOWLEDGEMENTS

We thank Jason Marcinkoski for his support of this work and his insightful feedback. This work was authored by Alliance for Sustainable Energy, LLC, the Manager and Operator of the National Renewable Energy Laboratory for the U.S. Department of Energy (DOE) under Contract No. DE-AC36-08GO28308. Funding provided by U.S. Department of Energy Office of Energy Efficiency and Renewable Energy Fuel Cell Technologies Office. The views expressed in the article do not necessarily represent the views of the DOE or the U.S. Government. The U.S. Government retains and the publisher, by accepting the article for publication, acknowledges that the U.S. Government retains a nonexclusive, paid-up, irrevocable, worldwide license to publish or reproduce the published form of this work, or allow others to do so, for U.S. Government purposes.